36992 PDF

Textile Structures for Composites

Project Code: S92-12

PI(s): Auburn: Sabit Adanur, Yasser Gowayed

Clemson: Mike Drews, B. Goswami, C. Huey, G. Lickfield

GA Tech: S. Kumar, R. Parachuru, Y. Wang

NCSU: Aly El-Shiekh, M. Mohamed (Project Leader), C. Pastore

Compiled By: Mansour H. Mohamed, NCSU

ANNUAL REPORT:

OBJECTIVES:

The overall objective of this work is to expand the boundaries of textile processing with the ultimate goal of producing new multi-dimensional fibrous structures for composite application.

Long Term:

1. The application and development of textile preforms' manufacturing methods by laminated and stitched fabrics, 2-D and 3-D braiding, 2-D and 3-D weaving, and warp and weft knitting.
2. To produce composites from these complex textile structures using different infiltration and consolidation systems.
3. To develop and validate analytical techniques for understanding the behavior of the composites as a function of process and reinforcement structure.
4. To develop a processing science and technology basis for the manufacturing of these materials and to develop an understanding of the interaction between processing performance.
5. To develop a "performance map" of the different textile reinforcement structures in terms of mechanical properties, shape forming capabilities, and eventually, economics to be used as a design guide for their application in end-use products.

SUMMARY:

This project is a joint effort between Auburn University, Clemson University, Georgia Tech and North Carolina State University. The faculty are divided into teams for fabrication, consolidation, analysis and testing.

The following preforms made up E - glass fibers were used: (1) [0/90] biaxial laminates; (2) [9/90] laminates interlocked by weaving in through-the-thickness direction or so-called 3-D woven samples (ratio of yarn in wrap/filling/z direction was 0.32/9.184/-.035; (3) 2-D woven [0/90] fabrics; (4) 2-D woven [0/90] fabrics stitched through-the-thickness. The 2-D woven fabric was plain weave with ratio of warp to fill yarns being approximately 1.3:1, Through-the-thickness machine stitching of the 2-D woven preforms was both uniaxial and biaxial using Kevlar^{TM} yarn with stitching lines being 5 or 10 mm apart. The reinforcement was impregnated with low-viscosity epoxy bisphenol F resin, Shell Epon^{R} DPL 862 mixed with the curing agent W, in a steel mold. The Resin Transfer Molding (RTM) machine VRM 2.5 from Liquid Control Corp. was employed for the resin impregnation. For comparison, samples were also made using hand lay-up in the same steel mold. Impregnated preforms were cured at 130^{o} C for 6h. The fiber volume fraction was about 55% in the laminate panels, and from 45 to 60% in the 2-D woven panels. Void content in the RTM panels was about 1.5 to 2% and in the hand lay up panels about 1 to 3.5%. The cured panels were cut into the testing coupons using a diamond abrasive blade. All the woven composite samples were tested along the warp yarn direction.

In addition to the standard coupon specimens, so-called mini-sandwich specimens were also fabricated [13]. The mini-sandwich specimen consisted of an epoxy core and single layers of the impregnated woven fabric placed on the top and bottom surfaces of the epoxy core (Fig.1). Tabs made of glass/epoxy were attached both to

the coupon and to the mini-sandwich specimens to set the configuration standardized for IITRI. In present study, 40 mm wide specimens were used (both in static compression and compression after impact) rather than standard 10 mm used in IITRI test. Comparison on composite made from woven fabric indicated that the compressive strength was insensitive to the width variation (40 mm vs. 10 mm).

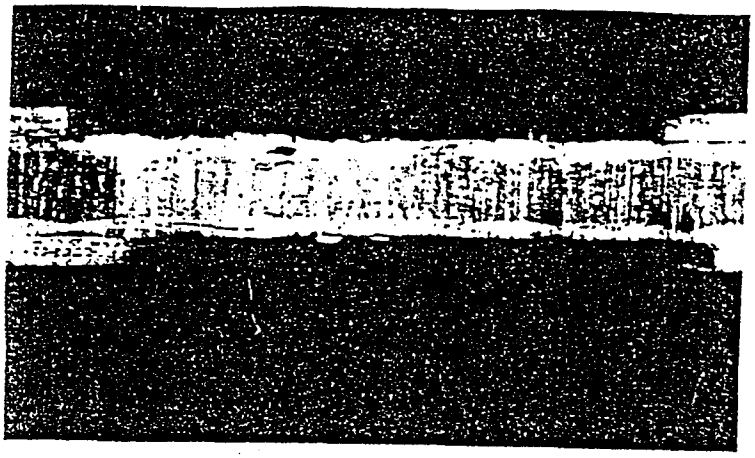

Figure 1. Photograph of the mini-sandwich specimen.

Low-velocity impact was applied to the tabbed coupons using a small pendulum apparatus [14]. The diameter of hemispherical impactor was 6 mm. The impact energy ranged from 0 to 8.7 J that corresponds to the energy of 0 to 2.5 J per 1 mm of the coupon thickness. Impact loading produced near-round damaged area. To compare CAI-strength and static open-hole compressive strength, the coupon specimens were drilled with approximately the same diameter hole as the diameter of the 3.6 J impact damage (13 mm).

The compressive stress-strain plots for both woven and laminate composites exhibit only slight nonlinearity (Fig. 2). Observed compressive failure modes in the laminate, and in the 3-D woven composites are given in Figure 3. The laminates fails via delamination (Fig. 3a). Similar structure laminates but woven in the through the thickness direction do not delaminate, but instead exhibit shear-like failure at 45^{o} (Fig. 3b). Such shear failure mode is considered to be fiber-strength dominated one [15]. Summary of the compressive strength data is given in 1. Obviously, relatively low strength values correspond to the delamination failure mode (438 MPa) as compared to the fiber-strength dominated mode (630 MPa). The small fiber content in through-the-thickness direction (3.5 vol%) significantly increases the laminate compressive strength. The choice of test (IITRI coupon vs. mini-sandwich) and fabrication (RTM vs. hand lay-up) techniques can be seen to have no influence on static compressive strength of the 2-D woven composites (Table 1).

Post-failure examination of the 2-D woven composite coupons revealed cracking in the $23\text{-}39^{o}$ range to the loading axis (Fig. 4). It is important to distinguish between initiation of compressive failure and post-failure phenomena. In order to pinpoint the failure initiation, the loading was stopped at 90-95% of the failure load. Compressive fracture was observed to initiate in the [0^{o}] warp yarn. More detailed information about the failure initiation was obtained from the testing of mini-sandwich specimens as only single fabric layers were located on the surface. The kink-like localized fractures were recorded to occur periodically along the crimped [0^{o}] yarns at the maximum misorientation points A (Figs. 5 and 6). The similar finding was reported for woven carbon/polymide composites [10] using IITRI test.

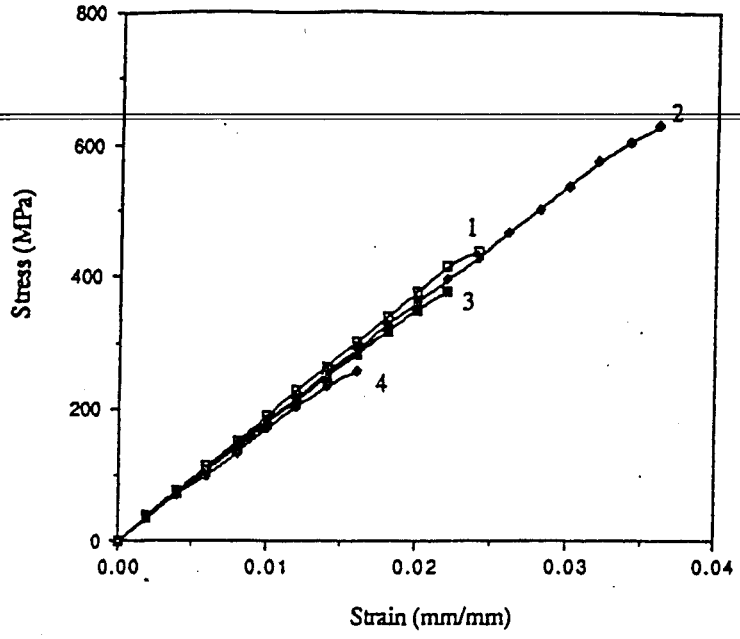

Figure 2. Compressive stress-strain plots of various composites. (1) 2-D laminate, (2) 3-D woven, (3) 2-D woven, and (4) stitched woven.

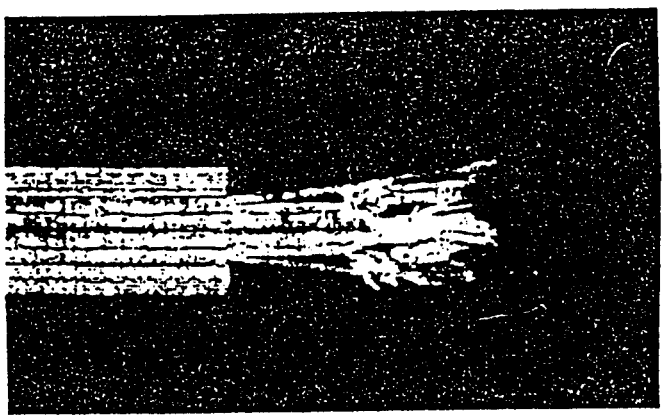

a. Delamination failure mode in glass/epoxy [0/90] laminate.

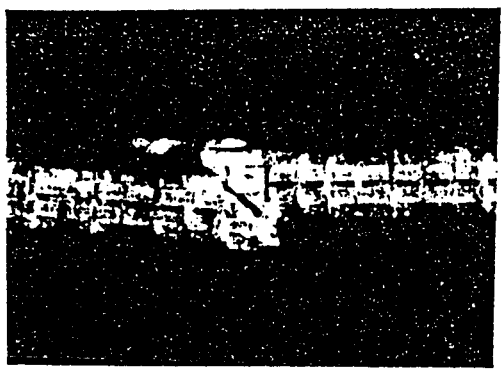

b. Shear failure in 3-D woven glass/epoxy laminate.

Figure 3. Compressive failure modes observed in the woven and laminate composites

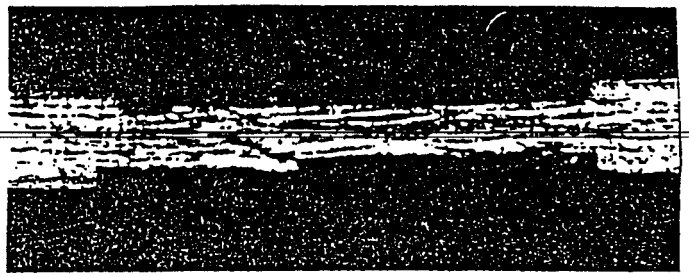

Figure 4. Compression failure in 2-D woven glass/epoxy composite.

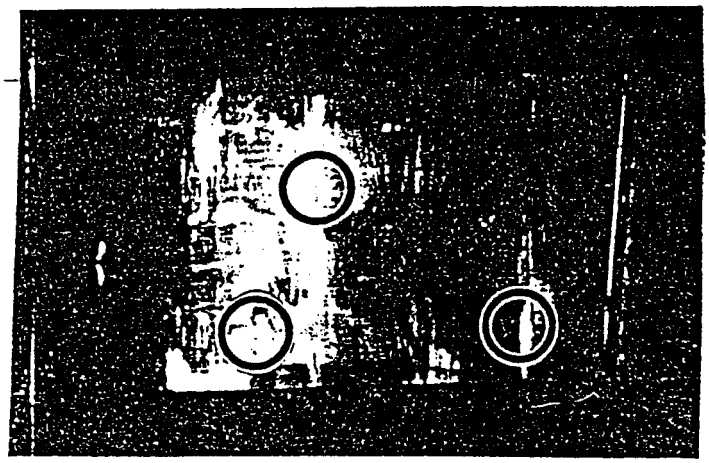

Figure 5. Localized fracture in the 0° wrap yarns under compression.

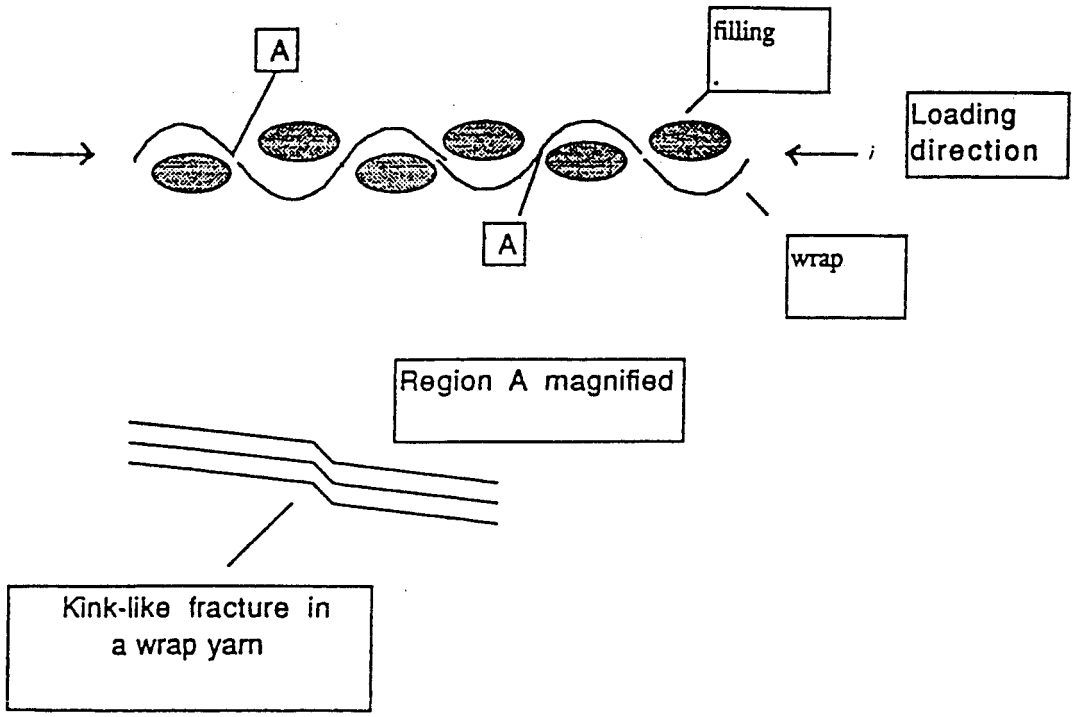

Figure 6. Schematic of compressive fracture in 2-D woven composites.

Two theoretical models proposed to predict compressive behavior of unidirectional composites [17, 18], can also be applied for woven composites. According to one model, compressive failure is via "in-phase" or "out-of-phase" buckling of perfectly aligned fibers or yarns, and compressive strength is given by the following formula [16]:

$$\alpha=G_m/(1-V_f) \quad \text{for "in-phase" buckling} \quad (1a)$$

$$\alpha=2[E_fE_m/3(1/V_f-1) \quad \text{for "out-of-phase" buckling} \quad (1b)$$

where V_f is the fiber volume fraction in the loading direction; E_f and E_m are the moduli of elasticity of fiber and matrix respectively, and G_m is the matrix shear modulus.

Two experimental findings about the tested woven composites are not consistent with the buckling model. First, compressive strength of the woven composites did not depend on fiber fraction ranged from 46 to 61vol%. Second, despite the fact that both "in-phase" or "out-of-phase" arrangements of individual woven fabric layers were observed on the surface of the woven composite specimens, the strength was the same.

The second theoretical model is the "fiber misalignment" model proposed by Argon [17]. Compressive failure is via kinks triggered in the region of fiber misalignment, and the compressive strength is given by [17]:

$$\alpha=\tau_c/\phi \quad (2)$$

where τ_c is the shear strength of composite; ϕ is the fiber misalignment angle.

The maximum misorientation in the warp yarns was measured to be about 5 to 7^O from the loading axis. The shear strength of the tested 2-D woven glass/epoxy composites varies from 32 to 40 MPa[14]. Substituting these figures into equation (2), one obtains compressive strength values in the 320 to 400 MPa range, which are in reasonable agreement with the experimental data given in Table 1.

Table 2 summarizes the data on Compression-After-Impact (CAI) and open-hole compression of the 2-D woven composites. Low-velocity impact of semi-spherical hammer generates approximately round-shape delamination damage area (Fig. 7). The damage area is approximately proportional to the impact energy. Similar results have been reported for carbon fiber laminates [18]. CAI strength of the woven glass/epoxy composites falls significantly as the impact energy is increased. CAI fracture was observed to occur in the impact damage cross-section (Fig. 8).

One can apply the linear elastic fracture mechanics (LEFM) theory to characterize the effect of the damage size D (i.e. the delamination crack size) on CAI strength. According to this theory, CAI strength is given by:

$$\alpha=K_1/(\pi D)^{1/2} \quad (3)$$

where K_1-stress intensity factor.

Last column in Table 2 shows that using the experimental values of σ and D, one can obtain approximately constant values of the stress intensity factor K_1 in full accordance with the LEFM. LEFM, therefore, accounts for the effect of impact damage size (and hence the impact energy) on CAI strength for the woven composites. It seems however that real CAI fracture micromechanism is more complex than envisioned by LEFM. For example, it has been observed that CAI-failure includes not only the macrocracking originating near the edge of the impact-induced delamination defect, but also numerous local fractures in $[O^O]$-yarns which were located in the volume of the material above and below the delamination defect. Besides, some sort of Euler post-buckling of the surface ply was sometimes observed to have developed above the delamination defect. Impact-induced damage area probably consists of numerous disc-shape delamination cracks located at different distances from the specimen surface, rather than a single crack assumed in the LEFM theory. The compressive strength of the woven glass/epoxy composites with an open hole is 35% lower than for the same-size impact-induced delamination defect (Table 2, compressive strength values of 153 vs. 236). Closely packed stitching improves the delamination resistance as shown in Table 3.

Table 2. CAI strength and open-hole compressive strength of woven [0/90] glass/epoxy composites

Material	Test	Compressive strength σ (MPa)	Damage area S (mm²)	Average damage diameter D (mm)	σ(π D)^1/2 (MPa mm^1/2)
2-D woven	CAI energy of impact=				
	0 J	398	-	-	-
	3.6 J (1 J/mm)	236	202	13.3	1530
	5.8 J (1.65J/mm)	202	320	15.8	1420
	8.7 J (2.5 J/mm)	186	480	21.4	1525
2-D woven	Open-hole	153	-	12.7	-

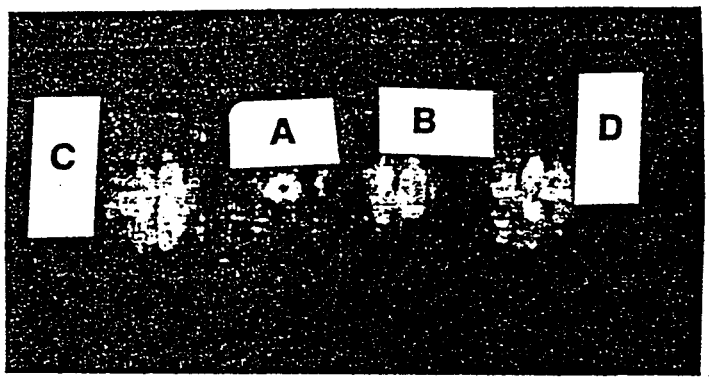

Figure 7. Impact damage in the 2-D woven glass/epoxy composite at various impact energy levels. (A) 1.1 J, (B)3.6 J, (C) 5.8 J, (D) 8.7 J

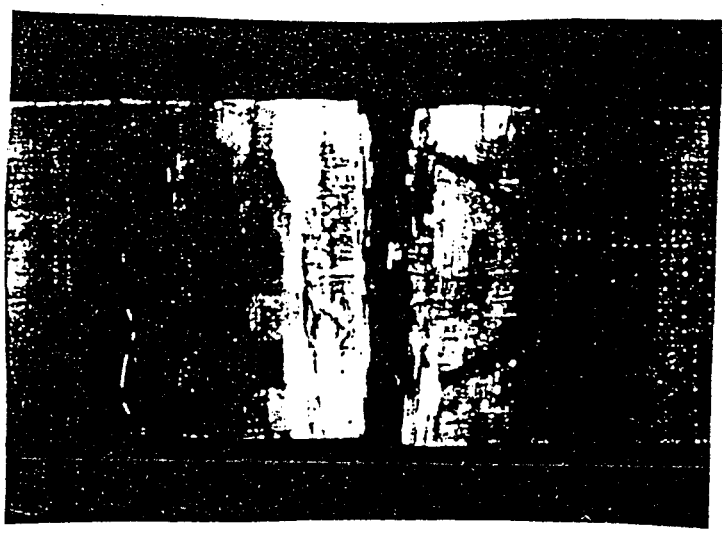

Figure 8. Compression-after-impact fracture in the 2-D woven glass/epoxy composite.

Table 3. Influence of stitching density on the delamination area after impact in 2-D woven glass/epoxy composite (z-direction stitching yarn is Kevlar™)
(6 layers of glass fabric)

Material	Relative Delamination Area
unstitched	100%
uniaxial stitching lines 10 mm apart	96%
biaxial stitching lines 10 mm apart	100%
uniaxial stitching lines 5 mm apart	79%
biaxial stitching lines 5 mm apart	75%

Two types of fiberglass yarns were used for comparison purpose, one without twist and the second twisted. 3-D woven panels were produced and composite were made for testing. The test results are shown in Table 4. It can be seen when there is some reduction in the properties of the composites. However, some of this reduction is due to the difference in fiber volume fractions between the two materials.

A project to evaluate the use of thermoplastic matrix in conjunction with weft knitted structures had the following objectives:

a) manufacturing of thermoplastic prepregs using friction spinning with glass fiber reinforcement and thermoplastic polyester staple fiber serving as the matrix in the subsequently processed composite parts,

b) processing of circular jersey knits using both friction spun yarn (glass/PET) and plain glass fiber roving,

c) fabrication of flat panels, tubes and T-shapes by autoclave molding using friction spun glass/polyester knit fabrics,

d) fabrication of flat panels by RTM using glass fiber knit,

e) characterization, evaluation and comparison of glass/polyester knit and glass/epoxy knit by selecting appropriate analytical test methods.

Composite parts processing

Thermoset Matrix Processing:

Preform: circular jersey knit, glass fiber roving, 136 text EC9 136 Z28 TD 22 (Vetrotex)

Matrix: Epon Resin DPL-862 & EPON Curing Agent W (Shell Chemical Company)

Processing: impregnation by RTM curing by autoclave processing: 8 hrs. at 250°F, 105 psig

V_f: 51-53%

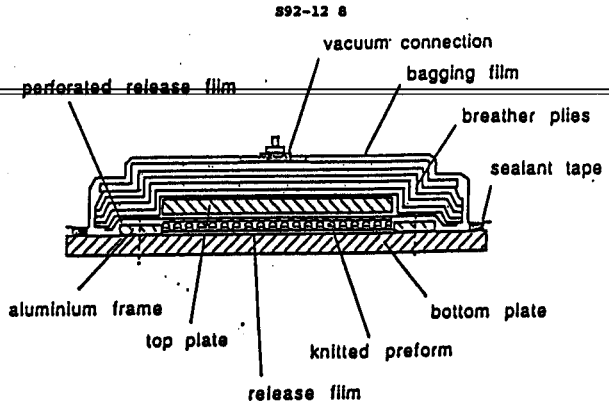

Figure 9: Thermoset Matrix Processing

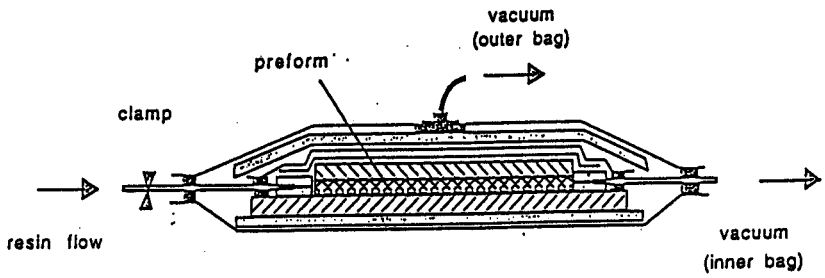

Figure 10: Thermoplastic Matrix Processing

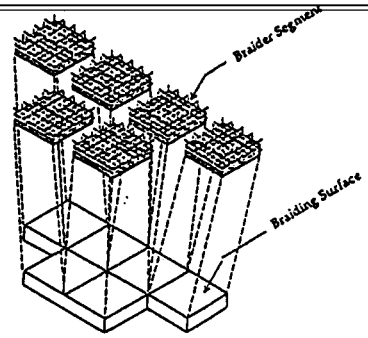

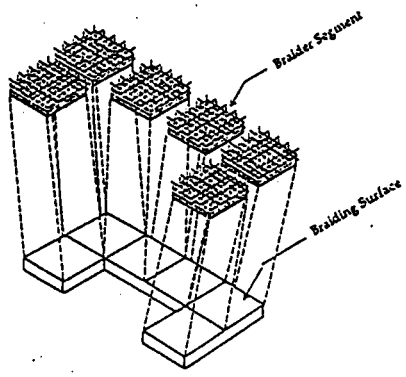

Figure 11: Alternate Arrangements of The Same Braider Segments to Yield a Brading Surface Having a Different Overall Configuration

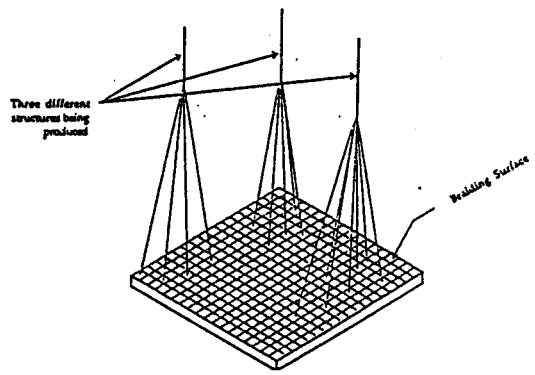

Figure 12: Braider Producing Several Structures Simultaneously

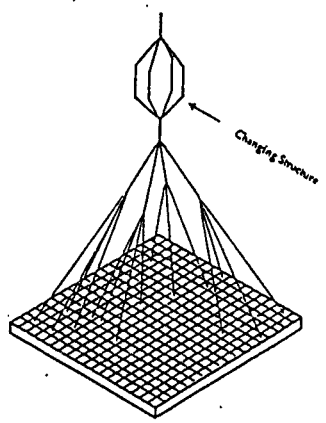

Figure 13: Braider Producing a Continuously Varying Structure

Table 4. Test Restuls on 3-D Woven Fabric Reinforced Composites

Matrix: Epon DPL 862/Curing Agent W
Woven Structure: 3D weave, 0.125" thickness

Test Type	*Material Constants*	*3D Woven, Untwisted Yarn*		*3D Woven, Twisted Yarn*	
		Longitudinal	*Transverse*	*Longitudinal*	*Transverse*
V_f		53.0%	53.0%	47.7%	47.7%
Tension	E(GPa)(% CV)	25.4 (6.48%)	24.0 (5.92%)	20.0 (0.7%)	18.6 (4.6%)
(Gage L=4")	S(MPa)(%CV)	399 (14.8%)	357 (5.33%)	347 (2.8%)	281 (5.7%)
	Nu	0.155	0.137	-	-
Compression	E(GPa)(% CV)	20.6 (3.11%)	18.6 (4.14%)	14.3 (1.6%)	12.1 (1.0%)
(Gage L=1")	S(MPa)(%CV)	425 (5.39%)	398 (2.07%)	358 (2.7%)	303 (2.7%)
Bending	E(GPa)(% CV)	12.4 (7.20%)	18.1 (4.52%)	15.4 (0.7%)	15.6 (3.3%)
(L/t=16, 3 pt)	S(MPa)(%CV)	507 (5.60%)	664 (4.50%)	456 (0.4%)	439 (3.5%)
Short Beam	Sb(MPa)(%CV)	312 (2.04%)	346 (3.88%)	396 (2.2%)	403 (3.0%)
Shear (L/t=4)	Ss(MPa)(%CV)	45.0 (2.47%)	51.9 (3.69%)	50.6 (2.1%)	51.4 (1.1%)

E=modulus, S=strength, nu=Poisson's Ratio
Sb=max bending stress, Ss=maximum shear stress (apparent interlaminar shear strength)

All specimen thickness=1/8" (nominal), about 3.5mm (actual). Specimen width=25.4 mm (1")

6 specimens tested for composite with untwisted yarn, 3 specimens for that with twisted yarn

Mechanical Tests

Several short term mechanical tests, such as tensile tests, three point flexure tests, and short beam shear tests were carried out to determine some of the basic material data, which ware widely used to rank materials for composite application.

	glass/PET jersey knit (0°/90°)	glass/epoxy jersey knit (0°/90°)
Short Beam Shear Test ASTM D-2344		
Shear strength [MPa]	27.9 / -	44.2 / -
Tensile Test ASTM D-3039		
Strength [MPa]	146 / -	192 / -
Modulus [GPa]	10.4 / -	12.16 / -
Three Point Flexure Test ASTM D-790		
Strength [MPa]	221 / 128.5	320 / 171
Modulus [GPa]	17 / 12	18.2 / 12.4
Strain [%]	2.34 / 2.31	2.93 / 2.41

The results indicate that microscopic images of laminate cross sections have shown good laminate quality, however there are resin rich areas in between sectors with high fiber volume fraction.

Jersey knits show fairly high anisotropic mechanical properties in tensile and flexural testing. Both strength and stiffness are increased when wales were oriented in specimen length axis (0^o). The mechanical properties of glass/epoxy knits are stronger and slightly stiffer than glass/PET specimen. This was to be expected due to the highly cross linked structure of thermoset matrixes.

Strength and stiffness were compared to various other reinforced plastics. Even in 0^{o} direction, both jersey knits show significantly lower tensile strength than for example woven glass/epoxy composites with similar fiber volume contents. In literature the tensile strength of a plain woven glass/epoxy is given with 425 MPa, the one for 2/2 twill with 570 MPa. Tensile modulus for these materials are within range of 18-20.5 MPa. Strength and stiffness of both jersey knits is superior or equal to SMC (30% glass fiber reinforced, wt), in 0^{o} direction, but lower in 90^{o} direction. Values for tensile strength and modulus of SMC, given by literature, were 183 MPa and 17.2 GPa respectively. In tensile testing SMC, however, shows very low breaking strain of 0.3-0.5%.

Thus jersey knits are not suitable for structural applications. If their anisotropic properties are considered, they may, however, be suited for some semi structural applications, especially when high preform drapeability is required.

Braiding research includes several project:

The prototype shuttle plate braider is now fully operational. Control software has been developed and all electro-mechanical components have been tested. The capacity of the machine remains limited by the small number of shuttles (six) that have been fabricated so far. An additional five are now under construction and will enable the production of more complex braids. The number of shuttles that can be accommodated is very large and more will be constructed if needed to complete the current development effort. The software component of the user/machine interface is being improved and hardware refinements are under way. A variety of samples have been produced to demonstrate the capabilities of the machine.

Assessment of Potential for the Shuttle Plate Braider

The shuttle plate process affords individual and independent control of each yarn being braided. Consequently, it can generate any structure that can be obtained by the interweaving of individual yarns. The capability of a single machine ranges from the emulation of simple processes such as weaving to the production of continuously changing, no-repeat, structural patterns. The machine can produce multiple items simultaneously. It is inherently modular, enabling the efficient matching of machine capacity to a particular structure. These features are indicated schematically in the attached figures.

In summary the new technology affords the following unique capabilities:

- Rapid production of prototypes of woven structures without the need for mechanical set-up
- Individual and independent control of each fiber thereby enabling continuously varying patterns to be produced
- Simultaneous production of several of the same or different items
- Emulation of any process, including simple and/or conventional ones, involving the interweaving fibers

Work on 3-D braiding has been concentrated in three areas. The first area focused on the development of a new and novel braiding process. 6-Step braiding combines the 4-step braiding process with an X-Y-Z structure by inserting filler yarns in the thickness, transverse, and longitudinal directions. A geometric model of the resulting preform was developed and used to establish relationships between the structural parameters.

The second area of research involved an evaluation of the compressive and flexural properties of composites. Comparisons were drawn between 3-D braided, triaxially braided and laminated composites. In addition, the effect of the presence of axial yarns in 3-D braids was also assessed. The results of mechanical testing (compression and four point bending) were related to preform architecture. The general conclusion was that property increases in one direction were accompanied by decreases in other directions. Specifically, the presence of axials in 3-D braids increased the longitudinal strength and modulus significantly.

The third area of research was a study of the bearing behavior of 3-D braided composite joints. Double lap joints were machined and tested in tensile loading to evaluate the effect of lateral constraint, bolt pitch, and hole pattern. The experiments supported existing theories on the benefits of lateral constraints and proper hole spacing.

Assembly of the multiaxial 3-D weaving machine is progressing and the machine is expected to be fully operational within the next two months. Patent application for this machine is pending.